

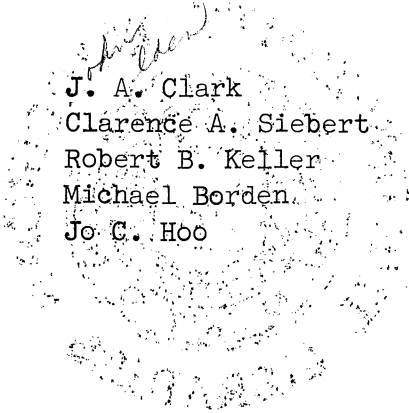
T H E U N I V E R S I T Y O F M I C H I G A N

COLLEGE OF ENGINEERING

Department of Mechanical Engineering
Heat Transfer Laboratory

Final Report

AUTOMOTIVE RADIATORS MANUFACTURED BY THE ELECTROFORMING PROCESS



J. A. Clark
Clarence A. Siebert
Robert B. Keller
Michael Borden
Jo C. Hoo

ORA Project 05335

under contract with:

INTERNATIONAL COPPER RESEARCH ASSOCIATION, INC.
NEW YORK, NEW YORK

administered through:

OFFICE OF RESEARCH ADMINISTRATION ANN ARBOR

December 1964

Engw

UMR

1314

4.2

TABLE OF CONTENTS

	Page
NOMENCLATURE	v
ABSTRACT	ix
1. INTRODUCTION	1
2. RESULTS, CONCLUSIONS, AND RECOMMENDATIONS	3
3. HEAT EXCHANGER DESIGN SELECTION AND TESTING	5
4. RESULTS	11
APPENDIX A. HEAT EXCHANGER ANALYSIS	15
1. Analysis	15
2. Reference Heat Exchanger and Reference Conditions	20
3. Heat Exchanger Matrices Studies	21
4. Heat Transfer and Friction Data	21
5. Results and Conclusions	21
APPENDIX B. RADIATOR HEAT TRANSFER PERFORMANCE TEST APPARATUS	27
1. Introduction	27
2. Heat Transfer Apparatus	27
3. Instrumentation for Heat Transfer Apparatus	28
4. Wind Tunnel	29
5. Instrumentation for Wind Tunnel	30
6. Wind Tunnel Development Tests	30
6.1 Bypass Performance	30
6.2 Test Section Velocity Distribution	31
7. Operating Experience and Procedures	31
7.1 Radiator Installation	31
7.2 Stabilization of Radiator Water Inlet Temperature	31
7.3 Typical Operating Procedure	33
APPENDIX C. METALLURGICAL STUDIES	35
1. Literature Survey of Solders	35
1.1 Tensile and Shear Strengths	35
1.2 Creep Properties	38
1.3 Fatigue Properties	39
1.4 Summary	40

TABLE OF CONTENTS (Concluded)

	Page
2. Literature Survey of the Mechanical and Physical Properties of Electroformed Copper	40
2.1 Summary	50
3. Tensile and Fatigue Test on Electroformed Copper	50
3.1 Conclusions	54
APPENDIX D. ELECTROFORMING PROCEDURES FOR HEAT EXCHANGER FABRICATION	55
REFERENCES	59

NOMENCLATURE

English

A	total heat transfer area on one side, ft ²
A _c	minimum air side free flow area, ft ²
A _{FR}	total frontal area air side, ft ²
a	plate thickness, ft
b	plate spacing, ft
c _p	specific heat at constant pressure, Btu/lbm-°F
f	friction factor, dimensionless
F	heat exchanger correction factor, dimensionless
G	mass velocity, (w/A _c), lbm/hr-ft ²
g _o	conversion factor; g _o = 32.2 (lbm/lbf) (ft/sec ²)
h	heat transfer coefficient, Btu/hr-ft ² -°F
k	thermal conductivity, Btu/hr-ft-°F
ℓ	length of fin, ft
L	total flow length of heat exchanger, ft
m	fin parameter, ft ⁻¹ , see Eq. (7)
NTU	number of transfer units, dimensionless
p	wetted perimeter of fin, ft
Pr	Prandtl number, dimensionless, see Eq. (9)
Δp	pressure drop, psf
q	heat transfer rate, Btu/hr

NOMENCLATURE (Continued)

English

Re	Reynolds number, dimensionless, see Eq. (10)
r_h	hydraulic radius ($A_c L/A$), ft, $4r_h =$ hydraulic diam
St	Stanton number, dimensionless, see Eq. (9)
t	fin thickness, ft
T	temperature, °F
ΔT_{OL}	log-mean temperature difference for pure counterflow, °F
U	overall heat transfer coefficient, Btu/hr-ft ² -°F
V	volume, ft ³
V_B	air volume between plates, ft ³
w	mass flow rate, lbm/hr

Greek

α	ratio of total heat transfer area on one side to total volume of heat exchanger A/V , ft ² /ft ³
β	ratio of total heat transfer area on one side of a plate-fin heat exchanger to the volume of air between plates on that side, A/V_B , ft ² /ft ³
δ	water channel thickness, ft
ϵ	heat transfer effectiveness (Ref. 1), dimensionless
η_o	total surface temperature effectiveness, dimensionless, see Eq. (5)
η_f	fin efficiency, dimensionless, see Eq. (7)
ϕ	A_c/A_{FR} , dimensionless
ρ	density, lbm/ft ³

NOMENCLATURE (Concluded)

Greek

μ	viscosity, lbm/ft-hr
ψ	see Eq. (32)

Subscripts

c	cold (air) side of heat exchanger
h	hot (water) side of heat exchanger
w	wall
max	maximum
min	minimum
i	inlet
o	reference heat exchanger.

Radiator Identification

EFHX-I	first model of a partially electroformed radiator (Figs. 6 and 9)
EFHX-II	second model of a partially electroformed radiator (Figs. 7 and 10)
SPHX	soldered radiator having physical characteristics similar to EFHX-I and -II. (Figs. 8 and 11)
LMHX	literature matrix heat exchanger (radiator) (Fig. 11).

ABSTRACT

This is the final report of a study to investigate the feasibility of manufacturing an automobile radiator (air-water heat exchanger) by the process of electroforming. It was concluded that owing to the present state of the technology of electroforming it is not economically practical at this time to fabricate radiators either partially or completely by the electroforming processes. The desirability of producing an electroformed radiator remains an important goal as such construction would eliminate the solder and could be expected to have superior strength, improved performance and higher reliability in comparison with conventional radiators.

It is recommended that further studies be undertaken to translate available information on transport phenomena in electrolytic systems to practical manufacturing processes. Significant improvement in industrial electroforming methods and techniques and the competitive position of this industry are considered possible by a careful and well planned application of transport theory.

Two partially electroformed radiators and one soldered radiator were designed, constructed and tested for their thermal and frictional pressure-drop performance. The first electroformed radiator displayed superior thermal performance and inferior frictional pressure-drop performance. This was attributed to an artificial surface roughness induced on the air-side surfaces by the processes of manufacture of the radiator and was not a direct consequence of the electroformed construction. Accordingly, further research was started on an investigation of the heat transfer characteristics of thin electroformed sheet which can be made with rough surfaces.

This report outlines the method of selection of the radiators for testing, the design and operation of a wind tunnel for radiator performance testing, test procedures and the results of the thermal and pressure drop testing of all radiators. These results are given in Appendices A and B.

A limited literature survey was made to obtain selected data on the mechanical properties of solders, soldered joints, and electroformed copper. Tensile and fatigue strengths were determined on nominal 0.010 and 0.020 inch thick strip specimens. The tensile strength averaged 27,818 and 27,324 psi respectively for these two average thicknesses. The endurance limit of these two nominal thicknesses based on ten million cycles was 11,500 and 10,500 psi respectively. These results are presented in Appendix C.

The electroforming procedures are presented in Appendix D and have been prepared by Mr. Frank K. Savage, President, Graham-Savage and Associates, Inc.,

Kalamazoo, Michigan. Mr. Savage was the consultant on electroforming manufacture processes and also supervised construction of all electroformed radiator subassemblies.

1. INTRODUCTION

This is the final report on "Automotive Radiators Manufactured by the Electroforming Process," a research program sponsored by the International Copper Research Association, Inc., New York, New York.

The objective of this study was to investigate the feasibility of manufacturing an automotive type radiator (air-water heat exchanger) wholly or in part by the process of electroforming. It was considered desirable from both an economic and performance reliability standpoint to eliminate the solder joints in presently manufactured radiators. To this end two partially electroformed radiators were assembled and performance tested in a wind tunnel designed for that purpose. Comparative performance of these partially electroformed radiators was obtained by testing a similar but soldered radiator and by using performance data from the standard literature on extended surface heat exchangers.

A partially electroformed heat exchanger was decided as a practical initial step in view of the state of the electroforming technology. This construction consisted of electroforming approximately 0.012 in. thick copper faces to the crests of pre-existent corrugated copper automotive radiator strip stock. Prior to electroforming the strip stock was encased in a melt-able alloy and the faces machined to expose to edges of the copper strip stock. The electroforming then completed a sub-assembly with two parallel faces connected laterally by the corrugated copper strip stock. Approximately twenty such subassemblies were soldered together to form the heat exchanger matrix with a 0.094 in. spacing between adjacent subassemblies serving as water coolant channels. Headers were attached at each end of the heat exchanger to provide for water coolant connection and distribution. Photographs of a typical subassembly and an assembled radiator (heat exchanger) are shown in Figs. 1 and 2. All electroforming operation were done by the Graham, Savage and Associates, Inc., Kalamazoo, Michigan, under the supervision of Mr. Frank K. Savage.

The heat exchanger design and testing were completed by The University of Michigan. This included the selection and evaluation of radiator core designs from the standpoint of their mechanical, thermal and frictional pressure drop performance, the selection of a specific design and a metallurgical study of the physical properties of electroformed copper sheets and electroformed copper joints. This latter involved a study of the microstructure characteristics and a determination of the tensile and fatigue strengths of the electroformed parts.

Mr. Richard D. Chapman, Director, Automotive Development, Copper and Brass Research Association, contributed to the general coordination of this work with interested parties in industry.

This report will be divided into two major parts. The first will be a brief summary of principal results, conclusions and recommendations, heat exchanger (radiator) design selection and testing, wind tunnel facility design, and experimental results. The second part consists of appendices in which much detailed information is presented on the summaries in the first part. The results of the metallurgical studies and the electroforming procedures are included as appendices.

An initial six-month progress report on this work was issued in May 1963 under the title "Automotive Radiators Manufactured by the Electroforming Process," some of the material from that report is reproduced here as appendices.

2. RESULTS, CONCLUSIONS AND RECOMMENDATIONS

Probably the most significant result of this research was the finding that with the current state of the technology of electroforming it is not economically feasible to manufacture an automotive radiator from partially electroformed sub-assemblies. Furthermore, in view of the complex geometry required for a heat exchanger of this type, i.e., extended surface on the air side, the technological problems of electroforming manufacture of the complete heat exchanger are themselves beyond the present level of this technology. The importance of an electroformed joint and consequent elimination of solder from these heat exchangers remains an important and desirable goal. Such a design could be expected to have superior strength, lighter weight and higher reliability in performance from both a thermal and leakage probability standpoint. However, it is apparent that as of today the practical problems of translating laboratory techniques of electroforming on relatively simple systems to the complex systems required in competitive, economic, quantity production have not been overcome.

In an independent study conducted by the principal author and one of his graduate students it has been found that an extensive literature exists on the mechanics of electroforming. Such work is usually focused on the laminar and turbulent transport processes in an electrolytic solution in the presence of an electric field. Probably for economic reasons this available body of scientific knowledge and techniques has not been extensively exploited in normal commercial electroforming operations.

Performance data on the thermal characteristics of the partially electroformed heat exchanger indicated a significantly superior heat exchange ability as compared with that of a soldered radiator. This was a result of an artificial surface roughness on the air side of the exchanger caused by a residue of the meltable alloy remaining on the surface subsequent to the removal of the alloy. This increased thermal performance was not believed to result from an improved thermal contact at the joint where the fin was attached to the water channel although photomicrographs confirmed that sound, metallurgically integral joints can be obtained. Such a possibility was discounted since the frictional pressure-drop for the electroformed heat exchanger also was greater than that of the soldered exchanger. A summary of the comparative thermal and frictional performance of all heat exchangers studied is presented in Fig. 3, 4 and 5. Nevertheless, this result pointed to the possibility of using relatively inexpensive, rough electroformed copper sheet stock as a material of construction for these types of heat exchangers in those circumstances where the disadvantages of loss in frictional characteristics are acceptable. The relative advantages of increased heat transfer from such roughened surfaces is currently being undertaken

by this laboratory under the present sponsor and results of a preliminary study are expected to be ready at the end of this year.

Apart from this investigation of the characteristics of rough electroformed surfaces, the following recommendation is made as a result of this study. There is at present an apparent information separation between the theoretical workers in electrochemistry and those in the transport mechanics of heat and mass transfer and the practitioners in the electroforming and electro-plating industry. As a consequence the electroforming technology has not been developed to the stage where it is practically possible nor economically feasible to electroform shapes as complex as those of an air-water heat exchanger. It has been found, however, that a great deal of useful information dealing with transport theory applied to electroforming processes is presently available, mostly in the form of scientific papers and monographs. This information ought to be carefully surveyed by competent and experienced personnel and a position paper formulated in a way which would be useful to application in the electrochemical industry. Such a study also would reveal areas in the technology of electro-deposition where additional investigation of the transport processes of heat and mass can produce potentially useful results. It is felt that significant improvement in industrial electroforming methods and techniques, and possibly the competitive position of this industry can be achieved by a careful and well-planned application of transport theory. In specific terms it is visualized that such an application would enable the prediction of rates of deposit (or removal) of metal on various geometric shapes in terms of electrolyte properties, flow rate, turbulence level, temperature, electric potential fields and diffusion coefficients, among others*. Such a study as is recommended here should include experimental investigations in circumstances having commercial importance but not be limited to these alone. New conditions of geometry, flow, electrolyte, potential field, etc., should be studied in order to investigate improved methods for the electroforming of new shapes. These results would apply as well to metal removing processes such as electro-chemical machining.

*It is recognized that surface phenomena not influenced by the transport processes will have an important effect on the deposition process and must be included in a comprehensive study.

3. HEAT EXCHANGER DESIGN SELECTION AND TESTING

At the start of this research it was desired to select a heat exchanger matrix for possible electroforming manufacture which would have thermal and frictional characteristics acceptable for automotive application and representative of that class of air-water heat exchangers. To accomplish this an optimization procedure was adopted which would select that heat exchanger matrix having the maximum rate of heat transfer per unit volume per unit frictional pressure drop. In other words, the matrix corresponding to this optimum would represent that design requiring the minimum volume and producing the minimum frictional pressure drop for a specified rate of heat transfer and air flow rate. The calculation of this optimum design required the use of experimental data on extended surface heat exchangers. The data employed were those published by Kays and London in Compact Heat Exchanger (1), an authoritative publication on this subject. The details of this optimization procedure and selection are outlined in Appendix A. As a result of this study it was determined that a matrix which was of a suitable optimum type on the basis of its thermal and frictional characteristics should be of a plate-fin design having 10 fins per in. with waviness, or turbulent promoters, on the fins. The air flow channel was to be between 0.40 and 0.50 in. wide, 2 in. deep and 12 in. in height, the latter two dimensions being selected arbitrarily. Such a design, it was felt, also would have a good chance of being fabricated, in part at least, by electroforming.

Three test heat exchangers were fabricated. All were essentially of the design shown in Fig. 2. Two of the exchangers were made of electroformed sub-assemblies and are referred to in this report as EFHX-I and EFHX-II (electroformed heat exchanger I and II). The third exchanger was basically the same, except that it was fabricated in a conventional manner by solder and is referred to here as SPHX (soldered prototype heat exchanger). For comparative purposes the experimental results from EFHX-I, EFHX-II and SPHX are compared with published results from the heat transfer literature on a similar heat exchanger matrix. This is identified as IMHX (literature matrix heat exchanger).

Both electroformed heat exchangers were manufactured from sub-assemblies such as that shown in Fig. 1. Pre-existent automotive radiator spacer stock was placed in a mold into which a meltable alloy was poured. After the alloy hardened it was removed from the mold and its lateral faces were machined exposing the thin edges of this copper spacer stock. This was then placed in an electrolytic bath and approximately 0.012 in. of copper was deposited on the machine faces forming a copper-copper joint with the spacer stock. The alloy was then melted out leaving a sub-assembly as shown in Fig. 1. Approximately 20 such sub-assemblies were placed adjacent to each other, separated

about 0.094 in. and soldered to form the basic heat exchanger matrix. Headers were attached at each end of the matrix to complete the heat exchanger. Detailed drawings of EFHX-I and -II are given in Figs. 6 and 7.

The soldered heat exchanger was assembled from the identical copper spacer stock as EFHX-I and -II. The air channels are wider in this design because the crests of the strip stock were not machined off. A detailed drawing of the soldered heat exchanger is shown in Fig. 8.

Detailed air-channel and water-channel dimensions as seen from the air flow direction are given in Figs. 9, 10 and 11 for EFHX-I, EFHX-II and the SPHX, respectively. The EFHX-I was fabricated by the Graham, Savage and Associates, Kalamazoo, Michigan. The EFHX-II was fabricated under the supervision of this laboratory using air channel sub-assemblies electroformed by the Graham, Savage and Associates and the SPHX was fabricated by the Young Radiator Company, Racine, Wisconsin. A summary of the principal geometric characteristics of each of these heat exchangers is given in Table 1.

The heat exchanger matrix referred to as LMHX is matrix number 11, Table 2 in Appendix A. This matrix was chosen for comparative purposes with the experimental data obtained in this study in order to provide an approximate independent check on the measurements obtained from EFHX-I, EFHX-II and the SPHX. The experimental data for LMHX were obtained by Kays and London and reported in Ref. 1. These data are reproduced here in Fig. 31.

The mechanical strength of an electroformed sub-assembly was tested by subjecting one of the electroformed faces to air pressure and measuring the corresponding deflection of the matrix. Air pressure was applied by the use of an air channel soldered to one side of the sub-assembly as shown in Fig. 12. This arrangement simulates the state of stress imposed on the matrix by the pressure of the water in the water channels. As may be observed from Fig. 12 the pressure-deformation characteristics are very complex as would be expected. Both elastic and plastic type behavior is seen with a certain amount of permanent deformation which increases at about 40 psig. However, even at a pressure of 60 psig, or about 4 atmospheres gage, the total deformation is only 0.038 in. The matrix was tested to 75 psig without rupture. On the basis of these results it was felt that the sub-assembly was of sufficient strength and rigidity for an automobile radiator. Designs having even greater stiffness can readily be fabricated.

The radiators were tested in a windtunnel specifically designed for this purpose. The wind tunnel, its auxiliaries, instrumentation and operating procedures are described in detail in Appendix B.

The rate of heat transfer q was determined from the enthalpy change of the heated water flowing through the core of the radiator. This enthalpy

TABLE 1

SUMMARY OF HEAT EXCHANGER CHARACTERISTICS*

SYMBOL	EFHX-I	EFHX-II	SPHX	IMHX
A, ft ²	38.8	35.3	38.4	—
A _c , ft ²	0.727	0.660	0.729	—
A _{FR} , ft ²	0.937	0.852	0.924	—
a, in.	0.012	0.012	0.010	—
b, in.	0.434	0.434	0.480	0.413
c, in.	0.002	0.002	0.002	0.006
L, in.	2.00	2.00	2.00	—
4r _c (airside), ft	0.01246	0.01246	0.01266	0.0106
4r _h (waterside), ft	0.01396	0.01509	0.01588	—
V, ft ³	0.156 ft ³	0.142	0.154	—
V _B , ft ³	0.1212	0.110	0.1215	—
α, ft ² /ft ³	249	248	249	294
β, ft ² /ft ³	321	321	316	351
δ, in.	0.094	0.094	0.099	—
σ,	0.776	0.775	0.789	0.836
A _w , ft ²	0.0251	0.0246	0.0271	—
A _h , ft ²	6.53	5.90	5.90	—
fins per in.	10	10	10	11.44

*Key

EFHX-I is the first electroformed heat exchanger fabricated (see Figs. 6 and 9)

EFHX-II is the second electroformed heat exchanger fabricated (see Figs. 7 and 10)

SPHX is the soldered heat exchanger (see Figs. 8 and 11)

IMHX literature heat exchanger (Fig. 31).

change was computed from measurements of the flow rate of the water and its temperature change. The objective of these tests was the determination of the average air-side heat transfer coefficient and the corresponding value of the Stanton number, the principal heat transfer parameter. Because of the test arrangement, the air-side heat transfer coefficient could not be obtained directly but had to be determined from indirect measurements and computations. The following is a brief description of the method of calculation of both the heat transfer and the frictional performance data.

The overall coefficient of heat transfer is determined from the rate equation for the radiator as,

$$q = \bar{U}AF \Delta T_{OL} = (wc_p)_h (T_o - T_i)_h \quad (1)$$

where,

ΔT_{OL} is the logarithmic mean temperature difference for pure counterflow.

F is the heat exchanger correction factor for the actual flow configuration (cross-flow, both fluids unmixed). In all cases F was approximately 0.99.

From Eq. (1) the product $\bar{U}A$ is written

$$\frac{1}{\bar{U}A} = \frac{F \Delta T_{OL}}{q} = \frac{F \Delta T_{OL}}{(wc_p)_h (T_o - T_i)_h} \quad (2)$$

also, by the definition of \bar{U} , we have

$$\frac{1}{\bar{U}A} = \frac{1}{\eta_{oc} h_c A} + \frac{a}{A_w k} + \frac{1}{\eta_{oh} h_h A_h} \quad (3)$$

however, for the radiator configurations employed the thermal resistance of the water channel wall is negligible and η_{oh} is unity. Hence,

$$\frac{1}{\bar{U}A} = \frac{1}{\eta_{oc} h_c A} + \frac{1}{h_h A} \quad (4)$$

the fin efficiency η_{oc} is given as

$$\eta_{oc} = 1 - \frac{Af}{A} (1 - \eta_f) \quad (5)$$

and

$$\eta_f = \frac{\text{Tanh}(ml)}{ml} \quad (6)$$

where,

$$m = \sqrt{\frac{hc p}{ktl}} \quad (7)$$

As may be noted from Eqs. (2), (4), (5), (6), and (7) the determination of hc , the average air-side heat transfer coefficient, requires values of h_h , the water side heat transfer coefficient. Furthermore, the air side fin efficiency η_{oc} itself involves hc . As a result once numerical values are obtained for h_h and UA , the final calculation of hc is a trial and error procedure. This computation is not difficult, however, since h_h is considerably greater than hc , in most cases, and the value of η_{oc} falls within fairly fixed limits. Numerical values for h_h were taken from the standard heat transfer literature for flow in channels.²⁵

The air side heat transfer data are presented in terms of the dimensionless parameters Stanton number, St , Prandtl number, Pr and Reynolds number Re . Data formulated in this manner provide a simple, meaningful and generalized method of presentation for comparative purposes. These results are summarized in Fig. 3 and are discussed below.

In addition to heat transfer data, measurements were taken of the frictional pressure drop characteristics of each radiator configuration. These results are summarized in Fig. 4 in terms of a friction factor f as a function of Reynolds number and are discussed below. The friction factor is given as

$$\frac{f}{2} = \frac{r_{cgo}\rho_o}{L} \left(\frac{Ac}{w_c} \right)^2 \Delta p_c \quad (8)$$

where,

Δp_c is the drop in total pressure across the radiator.

4. RESULTS

The experimental heat transfer and frictional pressure-drop results for the three radiators tested and the one taken from the literature are summarized in Figs. 3, 4 and 5. Individual results on each of the radiators are presented in Figs. 13 through 20.

Three experimental radiators were tested and an additional one of similar design was taken from the literature for comparative purposes. Physical property data on each of these radiators is summarized in Table 1. The radiators are identified as follows:

1. EFHX-I. First model of a partially electroformed radiator (Figs. 6 and 9)
2. EFHX-II. Second model of a partially electroformed radiator (Figs. 7 and 10)
3. SPHX. Soldered radiator having physical characteristics similar to EFHX-I and -II. (Figs. 8 and 11)
4. LMHX. Literature matrix heat exchanger (radiator) (Fig. 31).

Two partially electroformed radiators were fabricated as the first radiator was felt to be not of a sufficiently high standard of construction to be used for conclusive studies. In particular there were irregularities and excessive roughness in the air channel which would not be found in a commercial automobile radiator. Using the experience gained on the first, a second partially electroformed radiator was constructed and identified as EFHX-II. This radiator was assembled using electroformed sub-assemblies produced by Graham-Savage and Associates, Kalamazoo, Michigan. Its construction was done by soldering the sub-assemblies and was supervised by The University of Michigan. A completely soldered radiator (SPHX) was fabricated using the same spacer stock and tested for comparative purposes.

The heat transfer data are presented for the air-side as the product $St Pr^{2/3}$ as a function of the air-side Reynolds number Re_c . These dimensionless groups are defined as

$$St Pr^{2/3} = \frac{hc}{Gc_p} \left(\frac{c_p \mu}{k} \right)^{2/3} \quad (9)$$

$$Re_c = \frac{4r_c G}{\mu} \quad (10)$$

Friction data are given in terms of a friction factor f as a function of Reynold's number. These methods of representation generalize the data and allow for comparison between radiators as well as between various flow conditions for a given radiator. It also permits comparisons to be made without the requirement that air or water flow rates be identical for the comparison. In all data reported the Prandtl number was that for air and hence varied only slightly. Superior heat transfer performance among these essentially similar radiators is noted by a large $St Pr^{2/3}$ product for a given Reynold's number whereas superior friction pressure-drop performance would be indicated by small friction factor for a given Reynold's number.

The summary heat transfer data in Fig. 3 indicates that EFHX-I has superior performance to the others. Close inspection of the matrix disclosed a rough air-side surface condition which is believed to have caused an increase in the turbulence in the air-flow and thus the increased heat transfer. This is further borne out by the friction data summarized in Fig. 4 where EFHX-I also exhibits the greatest friction factor. This is consistent with the conclusion that air-side surface roughness is responsible for the increased heat transfer. The surface roughness is thought to be caused by a residue of the meltable alloy used to encase the copper spacer stock during the electroforming operation. Because of this it is concluded that the increase in heat transfer is not a result of improved performance owing to the electroformed copper spacer stock (fin) attachment to the water channel.

The heat transfer and friction characteristics of the other radiators are summarized in Figs. 3 and 4 also. Differences in the performance characteristics are less and the electroformed radiator (EFHX-II) exhibits somewhat better heat transfer and slightly poorer friction characteristics than the others, SPHX and LMHX. The soldered radiator (SPHX) has essentially identical heat transfer performance as the radiator matrix taken from the literature above a Reynold's number of about 1000. Its friction characteristics are generally superior to all other radiators, a probable result of its excellent manufacture.

Combined heat transfer and friction data for all radiators are presented in Fig. 5 as $St Pr^{2/3}/f$ as a function of the Reynold's number. Representation of this kind emphasizes both the heat transfer and friction characteristics of a radiator. Thus large values of $St Pr^{2/3}/f$ indicates both improved heat transfer and friction performance. As may be noted on this figure, the soldered radiator SPHX has superior performance while the first electroformed model EFHX-I exhibits the poorest performance. This latter is in line with the characteristics of EFHX-I as shown in Figs. 3 and 4. The heat transfer/

friction characteristics of EFHX-II and SPHX are about the same and each is superior to that of EFHX-I.

The heat transfer and friction data for each of the individual radiators are given in Figs. 13 through 20. Each data point corresponds to a separate run having a different water velocity. All tabulated data are on file with the principal author.

APPENDIX A

HEAT EXCHANGER ANALYSIS

1. ANALYSIS

The selection of the type of heat exchanger matrix suitable for an automotive radiator begins with an examination of the performance characteristics of typical existing air-water heat exchanger cores. The determination of the performance characteristics depends on the availability of generalized basic friction and heat transfer data of an experimental nature. Probably the most recent and comprehensive data of this kind presently available are those of Kays and London published in their book Compact Heat Exchangers.¹ This study reports the heat transfer and friction characteristics of 88 different kinds of extended surface heat exchangers suitable for gas turbine (gas-to-gas) or automotive (air-to-water) application. From this group 17 different matrices were selected for study and their relative thermal and friction performance determined. An eighteenth core included for comparison is a McCord Corporation type "GN" Honeycomb core for which the heat transfer and friction data has to be estimated from the best available source. A brief presentation of the analytical procedures follows.

The heat-transfer rate q in a heat exchanger may be expressed as follows

$$q = \epsilon (wcp)_{\min} (T_{h_i} - T_{c_i}) , \quad (11)$$

in which ϵ is the heat transfer effectiveness.¹ The remaining symbols are defined in the nomenclature of this report. In this analysis the relative performance of air-water heat exchangers will be determined for the following conditions:

- a. q is fixed
- b. T_{h_i} is fixed
- c. T_{c_i} is fixed
- d. $(wcp)_{\min}$ is fixed
- e. $(wcp)_{\max}$ is fixed.

For the usual automobile radiator $(wcp)_{\min}$ corresponds to the air-side and $(wcp)_{\max}$ corresponds to the water-side. The effectiveness ϵ is determined by the flow arrangement, i.e., counter flow, cross flow, etc., and the ratio $(wcp)_{\min}/(wcp)_{\max}$.¹ Hence, with the specifications a to e above, it is evident from Eq. (11) that ϵ will be fixed for all possible matrix shapes for a heat exchanger of a given flow arrangement. As shown by Kays and London¹ under these circumstances ϵ will then be a function only of the NTU, known as the number of transfer units in a heat exchanger. Furthermore, the NTU is defined as

$$NTU = \frac{UA}{(wc_p)_{\min}} . \quad (12)$$

Thus, we may now conclude that the relative performance of air-water heat exchangers may be determined on the basis of a fixed NTU which for the imposed restraints becomes

$$(UA)_1 = (UA)_2 . \quad (13)$$

Now, if A is based on the air-side or finned-side of the exchanger, we have,

$$\frac{1}{UA} = \frac{1}{\eta_{oc} h_c A} + \frac{a}{A_w k} + \frac{1}{\eta_{oh} h_h A_h} . \quad (14)$$

For the usual automobile radiator the last two terms in Eq. (14) are negligible, i.e., the air-side controls, so,

$$UA = \eta_{oc} h_c A . \quad (15)$$

Dropping the subscript c as all symbols now refer to the air-side, we have from Eqs. (13) and (15)

$$(\eta_{oh} A)_1 = (\eta_{oh} A)_2 \quad (16)$$

where

η_o = total surface temperature effectiveness.

Hence, for purposes of comparison between various heat exchanger matrices at constant NTU, their relative volumes may be given as

$$\frac{V_1}{V_2} = \frac{(UA/V)_2}{(UA/V)_1} = \frac{[(\eta_{oh})(A/V)]_2}{[(\eta_{oh})(A/V)]_1} . \quad (17)$$

A similar formulation may be written in which a "reference heat exchanger" matrix is used for comparison between all the others. Designating this reference exchanger by the subscript o we have,

$$\frac{V}{V_0} = \frac{[(\eta_0 h)(A/V)]_0}{[(\eta_0 h)(A/V)]} \quad (18)$$

With this formulation, then, any other two matrices, say 4 and 8 may be compared on a volume basis by

$$\frac{V_4}{V_8} = \frac{(V/V_0)_4}{(V/V_0)_8} \quad (19)$$

Now, the heat transfer parameter, the Stanton number, the flow parameter, the Reynolds number are defined as

$$St = \frac{h}{Gc_p} \quad (20)$$

$$Re = \frac{4r_h G}{\mu} \quad (21)$$

so,

$$\frac{h_0}{h} = \frac{St_0 G_0}{St G} = \frac{(St_0)(w/A_c)_0}{(St)(w/A_c)} \quad (22)$$

which for constant air-side flow w , becomes,

$$\frac{h_0}{h} = \frac{St_0}{St} \cdot \frac{A_c}{A_{c0}} \quad (23)$$

Because the air-side flow is the same in all comparisons, the Prandtl number is constant. Basic heat transfer data are given in terms of $St \cdot Pr^{1/3}$. Thus,

$$\frac{St_0}{St} = \frac{(St \cdot Pr^{2/3})_0}{St \cdot Pr^{2/3}}$$

Hence, from Eq. (18) we have for a fixed A_{FR} , the frontal area of the heat exchanger,

$$\begin{aligned}
\frac{V}{V} &= \frac{(\eta_o)_o}{(\eta_o)} \left(\frac{St_o}{St} \right) \left(\frac{A_c}{A_{c_o}} \right) \frac{(A/V)_o}{(A/V)} \\
&= \frac{(\eta_o)_o}{(\eta_o)} \left(\frac{St_o}{St} \right) \frac{(A_c/A_{FR})}{(A_c/A_{FR})_o} \frac{(A/V)_o}{(A/V)} \\
&= \frac{(\eta_o)_o}{(\eta_o)} \left(\frac{St_o}{St} \right) \left(\frac{\sigma}{\sigma_o} \right) \left(\frac{\alpha_o}{\alpha} \right) \tag{24}
\end{aligned}$$

where

$$\sigma \equiv \frac{A_c}{A_{FR}} \quad , \tag{25}$$

$$\alpha = \frac{A}{V} = \beta \sigma \tag{26}$$

and

$$\beta = \frac{A}{V_B} \quad .$$

Kays and London¹ report corresponding values of St , Re , σ , and α for the first 17 of the 18 heat exchanger surfaces considered in this report. Since the total volume of the matrix is written as $A_{FR} \cdot L$, where L is the depth of the matrix in the air flow direction, Eq. (24) may also be written for fixed frontal area and total surface temperature effectiveness, as

$$\frac{L}{L_o} = \left(\frac{St_o}{St} \right) \left(\frac{\sigma}{\sigma_o} \right) \left(\frac{\alpha_o}{\alpha} \right) = \frac{V}{V_o} \quad . \tag{27}$$

The Reynolds number ratio is written for constant w and A_{FR} from Eq. (21) as

$$\frac{Re}{Re_o} = \frac{(r_h/r_{h_o})}{(\sigma/\sigma_o)} \quad . \tag{28}$$

For tube-fin matrices, σ is uniquely specified by the particular matrix under consideration. In the case of plate-fin designs the ratio σ depends on the thickness, δ of the water channel and is computed from

$$\sigma = \frac{1}{1+\delta/b} \quad . \tag{29}$$

In these calculations δ is taken to be 0.080 in.

The above relationships permit the relative comparison between the heat transfer matrices from the standpoint of their thermal characteristics. A second important basis for comparison is the relative frictional pressure loss. Entrance and exit pressure losses are not included in this. The frictional pressure drop is expressed as

$$\Delta p = f \frac{L}{r_h} \frac{(w/A_c)^2}{2g_0\rho} = f \frac{L}{r_h} \frac{1}{A_c^2} \left(\frac{w^2}{2g_0\rho} \right) . \quad (30)$$

Hence, for the various matrices having constant frontal area, the relative frictional pressure loss is

$$\frac{\Delta p}{\Delta p_0} = \frac{(f/f_0)(L/L_0)}{(r_h/r_{h0})(\sigma/\sigma_0)} . \quad (31)$$

The last type of comparison to be made combines both the relative heat transfer and the relative friction. This is on the basis of heat transfer per unit volume per unit pressure drop. On this basis a favorable exchanger is one which has a large value of this parameter. Thus defining,

$$\psi = \frac{(q/V)}{\Delta p} , \quad (32)$$

we have the formulation of the relative value of this parameter as

$$\begin{aligned} \frac{\psi}{\psi_0} &= \frac{(q/V)/\Delta p}{(q/V)_0/\Delta p_0} \\ &= \frac{1}{(L/L_0)(\Delta p/\Delta p_0)} . \end{aligned} \quad (33)$$

Equation (33) also may be regarded as the relative value of the heat transfer rate per unit volume to frictional pumping power corresponding to the conditions specified.

Comparison between the various matrices is made for the volume ratio (and depth ratio), Eq. (27), frictional pressure drop ratio, Eq. (31), and heat transfer per unit volume per unit frictional pressure drop ratio, Eq. (33). All are based on a reference heat exchanger for reference conditions, defined below.

The 18 matrices considered here consist of six tube-fins, nine plate-fins, two tube-banks and one Honeycomb type. The geometry and basic friction and heat transfer data of the first 17 are given in Figs. 21-37, taken from Kays and London.¹ The eighteenth is a McCord Corporation type "GN" Honeycomb replacement core having 1/4-in. square air passages, 2-1/4 in. long. Since basic heat transfer and friction data are not available for this matrix, its performance was estimated from data in Kays and London for a dimpled tube having approximately the same hydraulic diameter as the selected Honeycomb core.

2. REFERENCE HEAT EXCHANGER AND REFERENCE CONDITIONS

The reference heat exchanger is a plate-fin matrix having strip-fins and is the Kays and London surface designated as 1/8-15.2, indicating that it is made of 1/8 in. wide fins and has 15.2 fins/in. The width b of the air-flow channel is 0.414 in. In this report the reference heat exchanger is designated as surface 14 and its geometry and basic heat transfer and friction characteristics are given in Fig. 34.

In order to have a specific flow condition for which all comparisons may be made, the following are taken

$$\begin{aligned} \text{Air velocity} &= 10 \text{ ft/sec} \\ \text{Air temperature} &= 100^\circ\text{F} \\ \mu &= 1.285 \times 10^{-5} \text{ lbm/ft/sec} \\ \rho &= 0.071 \text{ lbm/ft}^3 \end{aligned}$$

Hence,

$$\begin{aligned} 4r_{ho} &= 0.1042 \text{ in.} = 0.00868 \text{ ft} \\ \sigma_o &= 1/(1+0.080/0.414) = 0.838 \\ \beta_o &= 417 \text{ ft}^2/\text{ft}^3 \\ \alpha_o &= \beta_o \sigma_o = (417)(0.838) = 350 \\ Re_o &= 4r_{ho} G_o / \mu = 4r_{ho} (w/A_c)_o / \mu \\ &= 4r_{ho} \rho V A_{FR} / \mu (\sigma_o A_{FR}) = 4r_{ho} / \sigma_o (\rho V / \mu) \\ &= (0.00868)(0.071)(10) 10^5 / (0.838)(1.285) \\ &= 572. \end{aligned}$$

From Fig. 34 corresponding to $Re_o = 572$ we find,

$$(St-Pr^{2/3})_o = 0.0155 ,$$

and

$$f_o = 0.093 .$$

3. HEAT EXCHANGER MATRICES STUDIES

A summary of the 18 heat exchanger matrices selected for study is given in Table 2.

4. HEAT TRANSFER AND FRICTION DATA

The computed data for heat transfer and friction including the matrix parameters of σ , α , and β and their relative values are summarized in Tables 3 and 4.

5. RESULTS AND CONCLUSIONS

The relative volume or relative depth, V/V_o or L/L_o , relative friction pressure drop, $\Delta p/\Delta p_o$, and the relative heat transfer per unit volume per unit pressure drop, ψ/ψ_o are plotted in Figs. 38-40. From these results it is possible to compare all of the 18 matrices according to volume, pressure drop, and heat transfer per unit volume per unit pressure drop. As is evident by inspection, matrix 7 has lowest pressure drop but largest volume. From Table 2 it will be noted that this matrix is of the plate-fin type and very open with only 5.3 fins/in. and the second lowest area to volume ratio. The heat transfer per unit volume per unit pressure drop for this matrix is, however, rather poor, which is a result of its open design. From the standpoint of compactness matrix 12 is especially outstanding. This matrix has the smallest volume of them all (Fig. 38), and the highest heat transfer per unit volume per unit pressure drop (Fig. 40), although its frictional pressure drop is only moderately favorable (Fig. 39). The round tube banks (16 and 17) suffer from high pressure drop and high volume and consequently have very poor heat transfer per unit volume per unit pressure drop. The Honeycomb matrix, 18, also shows up poorly from the standpoint of compactness. Its pressure drop is second lowest but its heat transfer performance is not significant compared with the plate-fin designs.

These results indicate the superiority of the plate-fin type of matrix from the standpoint of maximum heat transfer per unit volume, minimum weight, and probably minimum cost. The benefit of turbulence promoters obtained by deforming the fins (wavy) is evident. The penalty is, of course, increased pressure drop but compactness is gained.

TABLE 2

Summary of Heat Exchanger Matrices*

Matrix No.	Classification	Matrix Type	Keys and London	Fins/in.	Hydraulic Diameter, in.	A/V ft ² /ft ³
1	Flat tubes, continuous fins	Flat tube, plain continuous fin	9.68-0.87	9.68	0.1416	229
2	Flat tubes, continuous fins	Flat tube, ruffled continuous fin	9.68-0.87R	9.68	0.1416	229
3	Flat tubes, continuous fins	Flat tube, plain continuous fin	9.1-0.737-S	9.1	0.1656	224
4	Flat tubes, continuous fins	Flat tube, ruffled continuous fin	9.29-0.737-SR	9.29	0.1622	228
5	Flat tubes, continuous fins	Flat tube, ruffled continuous fin	11.32-0.737-SR	11.32	0.1382	270
6	Round tube, continuous fins	Round tube, continuous fin	8.0-3/8T	8.0	0.1430	179
7	Plate fin, plain fins	Plain fin, b = 0.470 in.	5.3	5.3	0.2420	161
8	Plate fin, plain fins	Plain fin, b = 0.823 in.	9.03	9.03	0.1828	222
9	Plate fin, plain fins	Plain fin, b = 0.418 in.	15.08	15.08	0.1052	348
10	Plate fin, plain fins	Plain fin, b = 0.250 in.	19.86	19.86	0.0738	424
11	Plate fin, wavy fins	Wavy fin, b = 0.413 in.	11.44-3/8W	11.44	0.1272	294
12	Plate fin, wavy fins	Wavy fin, b = 0.413 in.	17.8-3/8W	17.8	0.0836	432
13	Plate fin, strip fin	Strip fin, b = 0.414 in.	3/32-12.22	12.22	0.1343	292
14	Plate fin, strip fin	Strip fin, b = 0.414 in.	1/8-15.2	15.2	0.1042	350
15	Plate fin, Louvered fin	Louvered fin, b = 0.250 in.	14/-11.1	11.1	0.1214	278
16	Round tube bank	Staggered	S-1.50-1.25(S)	--	0.1980	80.3
17	Round tube bank	In-line	I-1.50-1.25(S)	--	0.1980	80.4
18	Honeycomb	1/4-in.-2-1/4 in.	---	--	0.1410	192

*Round tubes with circular fins not considered since for available basic heat transfer data, tubes are larger than 3/8-in. dia and area/volume ratio is less than 170. These would not complete with the above configurations.

TABLE 3

Heat Transfer Data

Matrix No.	$4r_h$	r_h/r_{ho}	σ	σ/σ_0	β	α	α/α_0	Re/Re_0	Re	St·Pr ² /s	St/St ₀	I/I_0
1	0.1416	1.36	0.697	0.833	229	229	0.655	1.655	935	0.0063	0.405	3.14
2	0.1416	1.36	0.697	0.833	229	229	0.655	1.655	935	0.0079	0.510	2.50
3	0.1656	1.59	0.788	0.941	224	224	0.640	1.690	967	0.0110	0.710	2.07
4	0.1622	1.55	0.788	0.941	228	228	0.654	1.65	945	0.0115	0.740	1.98
5	0.1382	1.33	0.780	0.930	270	270	0.771	1.43	820	0.0110	0.710	1.70
6	0.1430	1.37	0.534	0.637	179	179	0.511	2.15	1230	0.0095	0.611	2.04
7	0.242	2.32	0.855	1.02	188	161	0.460	2.28	1300	0.0059	0.380	5.83
8	0.1828	1.75	0.911	1.09	244	222	0.635	1.61	920	0.0061	0.384	4.48
9	0.1052	1.01	0.840	1.00	414	348	0.995	1.00	572	0.0085	0.547	1.83
10	0.0738	0.707	0.757	0.905	561	424	1.215	0.782	447	0.0110	0.710	1.05
11	0.1272	1.22	0.836	1.00	351	294	0.840	1.22	699	0.0170	1.10	1.07
12	0.0836	0.800	0.835	1.00	514	432	1.235	0.800	468	0.0172	1.11	0.730
13	0.1343	1.29	0.858	1.02	340	292	0.833	1.265	725	0.0175	1.13	1.090
14	0.1042	1	0.838	1	417	350	1	1	572	0.0155	1	1
15	0.1214	1.162	0.758	0.905	367	278	0.795	1.285	736	0.0140	0.905	1.26
16	0.1980	1.90	0.333	0.398	80.3	80.3	0.228	4.77	2730	0.0130	0.840	2.08
17	0.198	1.90	0.388	0.463	80.4	80.4	0.228	4.10	2350	0.0115	0.742	2.74
18	0.141	1.35	0.563	0.671	192	192	0.549	2.01	1150	0.00562	0.362	3.38

TABLE 4

Friction Data

Matrix No.	Re	f	f/f ₀	L/L ₀	r _h /r _{h0}	σ/σ ₀	ΔP/ΔP ₀	$\frac{L(\Delta P)}{\Delta P(\Delta P_0)}$	ψ/ψ ₀
1	935	0.023	0.247	3.14	1.36	0.833	0.685	2.15	0.465
2	935	0.035	0.377	2.50	1.36	0.833	0.832	2.08	0.480
3	967	0.036	0.387	2.07	1.59	0.941	0.535	1.108	0.904
4	945	0.042	0.452	1.98	1.55	0.941	0.614	1.218	0.822
5	820	0.042	0.452	1.70	1.33	0.930	0.621	1.056	0.946
6	1230	0.028	0.301	2.04	1.37	0.637	0.704	1.435	0.696
7	1300	0.016	0.172	5.83	2.32	1.02	0.423	2.465	0.405
8	920	0.023	0.247	4.48	1.75	1.09	0.633	2.835	0.353
9	572	0.036	0.387	1.83	1.01	1.00	0.705	1.290	0.775
10	447	0.041	0.441	1.05	0.707	0.905	0.725	0.741	1.350
11	699	0.092	0.990	1.07	1.22	1.00	0.869	0.930	1.075
12	468	0.083	0.893	0.730	0.800	1.00	0.815	0.595	1.680
13	725	0.100	1.075	1.090	1.29	1.02	0.891	0.971	1.030
14	572	0.093	1	1	1	1	1	1	1
15	736	0.070	0.753	1.26	1.162	0.905	0.900	1.135	0.880
16	2730	0.071	0.764	2.08	1.90	0.398	2.10	4.19	0.239
17	2350	0.053	0.570	2.74	1.90	0.463	1.78	4.88	0.205
18	1150	0.0125	0.1345	3.38	1.35	0.671	0.501	1.70	0.587

It was on the basis of these calculations that the matrix for the first electroformed model heat exchanger was selected. While matrix 12 is the most compact of the group it has a fairly high number of fins/inch—17.8. It was felt that for the first electroformed model the number of fins/inch ought not to exceed about 10 to reduce the electroforming problems and to have a design which is similar to current automotive practice. The model should however be of a plate-fin design with waviness in the fins, if possible.

